

A Closed-Form Expression for Estimating Radiated Emissions From the Power Planes in a Populated Printed Circuit Board

Hwan-Woo Shim, *Member, IEEE*, and Todd H. Hubing, *Senior Member, IEEE*

Abstract—An expression for the maximum intensity of radiated emissions from a rectangular power bus structure has been derived based on an analytical cavity-resonator model. The effect of components mounted on the board is modeled by modifying the propagation constant of the waves within the power bus structure. The radiated field intensity is calculated using the equivalent magnetic current around the edges of the power bus structure together with the modified propagation constant. Measurements of a populated test board show that the derived closed-form expression estimates the level of the maximum radiation intensity with reasonable accuracy.

Index Terms—Cavity model, decoupling, power bus noise, propagation constant, radiated emissions.

I. INTRODUCTION

TRANSIENT currents drawn by the active devices on a printed circuit board produce voltage fluctuations on the power bus. For high-speed digital systems, this power noise can be the source of significant radiated emissions, particularly when the power is distributed on planes [1]–[3]. To mitigate the direct radiation from power bus structures, several methods have been proposed. At frequencies below a few hundred megahertz, decoupling capacitors mounted to the board can reduce the power bus noise and the resulting emissions from the power bus [4]–[10]. At higher frequencies, embedded capacitance can be employed [11], [12], the planes can be connected together around their periphery with a resistive termination [13], or power planes can be located on layers between two ground planes that are stitched together using many vias [14].

Each of these methods to reduce emissions from a power bus structure has a cost associated with it in terms of board real estate, component costs, or manufacturing costs. In many cases, emissions directly from the power bus will not be high enough to create a problem. Therefore, measures to reduce power bus emissions should only be applied when the emissions are expected to be significant. Expressions for estimating the potential radiated field intensity from a power bus structure can help designers to anticipate potential problems and avoid unnecessary costs.

Recently, Leone developed a simple closed-form expression to estimate maximum radiated emissions from a rectangular

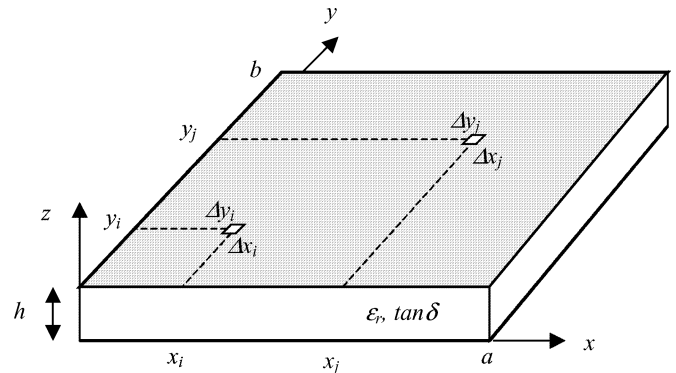


Fig. 1. Rectangular power plane pair.

power bus structure [16]. He used a cavity model [17]–[24] to get the field distribution along the edges. Then, the radiated fields were calculated using equivalent magnetic currents. The results showed that, near resonant frequencies, currents as low as a few milliamps could result in unacceptable radiated emissions. The model in [16] assumed a bare board without any components. In practice, most printed circuit boards are covered with components. The components may not be important for boards with closely spaced planes since the conductive loss of the copper planes damps resonances significantly [23]. Furthermore, the radiated emissions are not a concern for most thin boards, since the intensity of the radiated fields is proportional to the spacing between planes. However, the components can play an important role for thicker boards (e.g., plane spacings greater than a few hundred microns). For these boards, the effects of the components on the quality factor of the resonance must be taken into account. In this paper, the authors model power bus structures as cavities and modify the propagation constant within the cavity to account for the effects of the mounted components. Using the modified propagation constant, a new closed-form expression for the maximum radiated field intensity from a rectangular power bus structure is derived.

II. CAVITY MODEL OF A RECTANGULAR POWER BUS STRUCTURE

The structure under consideration is illustrated in Fig. 1. The spacing h between the two planes is assumed to be electrically small, so the structure supports modes that have only a vertical component of electric field E_z and tangential components of magnetic field H_x and H_y . This enables us to model the structure as a cavity by considering the edges to be perfect magnetic

Manuscript received January 7, 2005; revised September 24, 2005.

H.-W. Shim is with Samsung Corporation, Gumi-city, Korea (e-mail: hwanwoo.shim@samsung.com).

T. H. Hubing is with the Electrical and Computer Engineering Department, University of Missouri-Rolla, Rolla, MO 65409 USA (e-mail: hubing@umr.edu).

Digital Object Identifier 10.1109/TEMC.2005.861377

conductor (PMC) walls. Two ports are located at (x_i, y_i) and (x_j, y_j) that have electrically small rectangular cross sections of $(\Delta x_i, \Delta y_i)$ and $(\Delta x_j, \Delta y_j)$, respectively.

Since the magnetic fields are perpendicular to the z -direction, the fields inside the cavity can be expressed in terms of summations of modal functions of two-dimensional (2-D) TM_z modes. The transfer impedance between the two ports in Fig. 1 is given by [16]–[23] [see (1) at the bottom of the page], where $k_{xm} = (ma)/(\pi)$, $k_{yn} = (nb)/(\pi)$, and χ_{mn}^2 is given by

$$\chi_{mn}^2 = \begin{cases} 1, & m = n = 0 \\ 2, & m = 0 \text{ or } n = 0 \\ 4, & mn \neq 0. \end{cases} \quad (2)$$

The complex propagation constant γ can be written as [22]

$$\gamma = j\omega\sqrt{\varepsilon\mu}\sqrt{\left(1 - j\frac{(1+j)\delta_s}{h}\right)(1 - j\tan\delta)} \quad (3)$$

where δ_s is the skin depth in the plane conductors, $\tan\delta$ is the loss tangent of the dielectric substrate, and ε is the permittivity of the dielectric substrate. This expression for γ does not account for the radiation loss, which has a negligible effect on the fields between the plane in typical power bus structures [21]–[23]. If the dielectric material is reasonably low loss, (3) is approximately given by

$$\gamma \approx j\omega\sqrt{\varepsilon\mu}\left(1 - j\frac{\tan\delta + \delta_s/h}{2}\right). \quad (4)$$

If the dimensions of the ports are much smaller than those of the board, (1) can be simplified, as shown in (5) at the bottom of the page.

The electric field E_z at an arbitrary point (x_j, y_j) on the board can be written in terms of the transfer impedance Z_{ij} assuming a filamentary current source I_i at an arbitrary point (x_i, y_i) .

$$E_z(x_j, y_j) = \frac{1}{h}V(x_j, y_j) = \frac{1}{h}Z_{ij} \times I_i(x_i, y_i). \quad (6)$$

The radiated field from the rectangular power bus structure can be calculated using Huygens' Principle [25]–[27]. This principle says that the radiated fields exterior to a region including

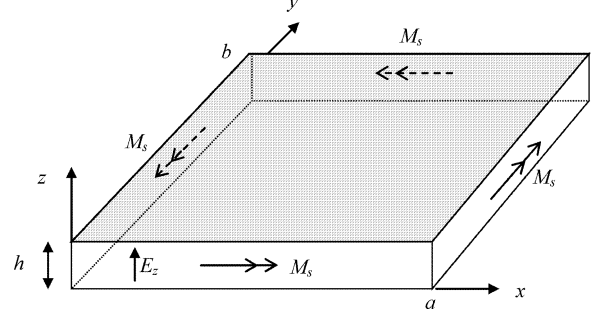


Fig. 2. Equivalent magnetic current on the periphery of the planes.

the sources can be determined by equivalent current sources on the boundary surface of the source volume. The equivalent current sources are related to the tangential components of the electric fields and the magnetic fields. The tangential magnetic fields can be neglected for a thin board, so the radiated field is determined by the tangential electric field on the edges. The corresponding equivalent magnetic current is given by [25]

$$\bar{M}_s = -\hat{n} \times \bar{E}_z \quad (7)$$

where \bar{E}_z is the tangential electric field at the edge openings and \hat{n} is a normal vector pointing out from of the board. The equivalent magnetic current is shown in Fig. 2.

Using the equivalent magnetic current as the radiation source, the far-zone radiated fields can be calculated using the free-space Green's function as [16], [25], [26]

$$\begin{aligned} \bar{E} &= \frac{h}{4\pi} \nabla \times \int_C \bar{M}_s(\bar{r}') \frac{e^{-jk_0|\bar{r}-\bar{r}'|}}{|\bar{r}-\bar{r}'|} d\ell' \\ &\approx j \frac{k_0 h}{4\pi} \frac{e^{-jk_0 r}}{r} \int_C \{\hat{r} \times \bar{M}_s(\bar{r}')\} e^{jk_0(\bar{r}' \cdot \hat{r})} d\ell' \end{aligned} \quad (8)$$

where the integral path C extends over the periphery of the board and \bar{r} and \bar{r}' are observation and source point vectors, respectively, expressed in spherical coordinates. Combining (5)–(8)

$$\begin{aligned} Z_{ij} &= j\omega\mu h \sum_{m=0}^{\infty} \sum_{n=0}^{\infty} \frac{\chi_{mnn}^2 \cos(k_{xm}x_i) \cos(k_{yn}y_i) \cos(k_{xm}x_j) \cos(k_{yn}y_j)}{ab(k_{xm}^2 + k_{yn}^2 + \gamma^2)} \\ &\quad \times \text{sinc}(k_{xm}\Delta x_i/2\pi) \text{sinc}(k_{yn}\Delta y_i/2\pi) \\ &\quad \times \text{sinc}(k_{xm}\Delta x_j/2\pi) \text{sinc}(k_{yn}\Delta y_j/2\pi) \\ &\equiv \sum_{m=0}^{\infty} \sum_{n=0}^{\infty} Z_{ij,mn} \end{aligned} \quad (1)$$

$$\begin{aligned} Z_{ij} &\approx j\omega\mu h \\ &\quad \times \sum_{m=0}^{\infty} \sum_{n=0}^{\infty} \frac{\chi_{mnn}^2 \cos(k_{xm}x_i) \cos(k_{yn}y_i) \cos(k_{xm}x_j) \cos(k_{yn}y_j)}{ab(k_{xm}^2 + k_{yn}^2 + \gamma^2)}. \end{aligned} \quad (5)$$

and evaluating the integral, the radiated field can be written as

$$\begin{aligned} \bar{E}_{M_x} \approx & \frac{k_o^2 \eta_o h I_i e^{-jk_o r}}{4\pi r} (\hat{r} \times \hat{x}) \\ & \cdot \sum_{m=0}^{\infty} \sum_{n=0}^{\infty} \left\{ \frac{\chi_{mn}^2 \cos(k_{xm} x_i) \cos(k_{yn} y_i)}{ab (k_{xm}^2 + k_{yn}^2 + \gamma^2)} \right. \\ & \cdot \frac{jk_o \sin \theta \cos \phi}{k_{xm}^2 - k_o^2 \sin^2 \theta \cos^2 \phi} \\ & \cdot [1 - (-1)^m e^{jk_o a \sin \theta \cos \phi}] \\ & \cdot \left. [1 + (-1)^n \cdot e^{jk_o b \sin \theta \sin \phi}] \right\} \end{aligned} \quad (9)$$

and

$$\begin{aligned} \bar{E}_{M_y} \approx & \frac{k_o^2 \eta_o h I_i e^{-jk_o r}}{4\pi r} (\hat{r} \times \hat{y}) \\ & \cdot \sum_{m=0}^{\infty} \sum_{n=0}^{\infty} \left\{ \frac{\chi_{mn}^2 \cos(k_{xm} x_i) \cos(k_{yn} y_i)}{ab (k_{xm}^2 + k_{yn}^2 + \gamma^2)} \right. \\ & \cdot \frac{-jk_o \sin \theta \sin \phi}{k_{yn}^2 - k_o^2 \sin^2 \theta \sin^2 \phi} \\ & \cdot [1 - (-1)^n e^{jk_o b \sin \theta \sin \phi}] \\ & \cdot \left. [1 + (-1)^m e^{jk_o a \sin \theta \cos \phi}] \right\} \end{aligned} \quad (10)$$

where \bar{E}_{M_x} and \bar{E}_{M_y} are far-zone electric fields due to the x and y components of the equivalent magnetic currents, respectively. E_θ and E_ϕ can be obtained by expanding the $(\hat{r} \times \hat{x})$ and $(\hat{r} \times \hat{y})$ terms in purely spherical coordinates and combining (9) and (10). The expressions for the radiated fields then become (11) and (12), shown at the bottom of page. Finally, the magnitude of the maximum radiated field is given by

$$|E| = \sqrt{|E_\theta|^2 + |E_\phi|^2}. \quad (13)$$

III. RADIATION INTENSITY FROM A BARE BOARD

The radiated field is proportional to the impedance Z_{ij} , which has local maximum values at resonant frequencies. These local maximum values are proportional to the Q factor of the resonance [23]. The Q factor is determined by various losses inside the structure. In general, the sources of loss in a bare board are conductive loss, dielectric loss, radiation loss, and surface wave loss. But the surface wave loss and radiation loss can be neglected for the purposes of estimating the interior fields, since they are usually small relative to the other losses for typical printed circuit board geometries [22]. The conductive loss dominates in power buses with closely spaced planes and the dielectric loss dominates when the dielectric layers are thicker [23]. In general, the dielectric material for a power bus structure is a relatively good insulator and has a low loss tangent. So, thicker boards without any components have relatively high quality factors. For example, the quality factor of a 0.5-mm-thick board made with FR-4 is about 40 at resonant frequencies [23]. For thicker boards without components, the Q factor approaches

$$\begin{aligned} E_\theta \approx & j \frac{k_o^3 \eta_o h I_i e^{-jk_o r}}{4\pi r} \\ & \cdot \sum_{m=0}^{\infty} \sum_{n=0}^{\infty} \left\{ \frac{\chi_{mn}^2 \cos(k_{xm} x_i) \cos(k_{yn} y_i)}{ab (k_{xm}^2 + k_{yn}^2 + \gamma^2)} \cdot \sin \theta \sin \phi \cos \phi \right. \\ & \cdot \left(\frac{[1 - (-1)^m e^{jk_o a \sin \theta \cos \phi}][1 - (-1)^n \cdot e^{jk_o b \sin \theta \sin \phi}]}{k_{xm}^2 - k_o^2 \sin^2 \theta \cos^2 \phi} \right. \\ & \left. \left. + \frac{[1 - (-1)^n e^{jk_o b \sin \theta \sin \phi}][1 - (-1)^m \cdot e^{jk_o a \sin \theta \cos \phi}]}{k_{yn}^2 - k_o^2 \sin^2 \theta \sin^2 \phi} \right) \right\} \end{aligned} \quad (11)$$

and

$$\begin{aligned} E_\phi \approx & j \frac{k_o^3 \eta_o h I_i e^{-jk_o r}}{4\pi r} \\ & \cdot \sum_{m=0}^{\infty} \sum_{n=0}^{\infty} \left\{ \frac{\chi_{mn}^2 \cos(k_{xm} x_i) \cos(k_{yn} y_i)}{ab (k_{xm}^2 + k_{yn}^2 + \gamma^2)} \cdot \sin \theta \cos \theta \right. \\ & \cdot \left(\frac{[1 - (-1)^m e^{jk_o a \sin \theta \cos \phi}][1 - (-1)^n \cdot e^{jk_o b \sin \theta \sin \phi}] \cos^2 \phi}{k_{xm}^2 - k_o^2 \sin^2 \theta \cos^2 \phi} \right. \\ & \left. \left. - \frac{[1 - (-1)^n e^{jk_o b \sin \theta \sin \phi}][1 - (-1)^m \cdot e^{jk_o a \sin \theta \cos \phi}] \sin^2 \phi}{k_{yn}^2 - k_o^2 \sin^2 \theta \sin^2 \phi} \right) \right\}. \end{aligned} \quad (12)$$

the inverse of the dielectric loss tangent and can be 50–100 or higher for common circuit board dielectrics.

If the separation between the two planes is very thin (i.e., comparable to the skin depth in the planes), the radiation intensity may generally be neglected since the field strength is proportional to the separation [16] and resonances will be efficiently damped [22], [23]. Therefore, the power bus radiation from a board with a plane spacing on the order of several microns can normally be neglected. In this paper, the thickness of the dielectric layer is considered to be much greater than the skin depth of the conductor such that conductive loss can be neglected.

For a high- Q resonances (e.g., $Q > 10$), the maximum radiated field is determined primarily by one mode if the source is located where that mode is excited. For TM_{m0} modes, the two equivalent magnetic current sources are located parallel to the y axis at $x = 0$ and $x = a$. The maximum E-field is E_θ on the x - z plane. The maximum intensity for TM_{m0} modes can be found by taking the limit as $\phi \rightarrow 0$ in (11) and combining the result with (4) yielding

$$\begin{aligned} |E_{TM_{m0}}|_{\max} &= \frac{\eta_0 h I_i}{2\pi \epsilon_r a r} \cdot \left| \cos\left(\frac{m\pi x_i}{a}\right) \right| \cdot Q_{\text{bare}}(f) \\ &\quad \cdot |1 - (-1)^m e^{jk_0 a \sin\theta}| \\ &\leq \frac{\eta_0 h I_i}{\pi \epsilon_r a r} \cdot \left| \cos\left(\frac{m\pi x_i}{a}\right) \right| \cdot Q_{\text{bare}}(f) \end{aligned} \quad (14)$$

where $Q_{\text{bare}}(f) = (Q_c^{-1} + Q_d^{-1})^{-1}$. Q_c and Q_d are the quality factors due to the conductive loss and dielectric loss, respectively and are given by [23], [25]

$$Q_d = \frac{1}{\tan\delta}, \quad Q_c = \frac{h}{\delta_s}. \quad (15)$$

Equation (14) is similar to (40) in [16], which was derived for the TM_{10} mode. This simple expression is valid not only for the first resonant frequency but also for the higher mode resonances. Similarly, the maximum field for TM_{0n} modes can be expressed as

$$|E_{TM_{0n}}|_{\max} \leq \frac{\eta_0 h I_i}{\pi \epsilon_r b r} \cdot \left| \cos\left(\frac{n\pi y_i}{b}\right) \right| \cdot Q_{\text{bare}}(f). \quad (16)$$

For TM_{mn} modes with $m \neq 0$ and $n \neq 0$, the phase of the equivalent magnetic current source alternates along each edge resulting in some cancellation of the radiated field components. This implies that the maximum field intensity of the TM_{mn} modes is less than that of the TM_{m0} or TM_{0n} modes.

Fig. 3 shows the calculated maximum field from a sample board. The input current is 1.0 mA and the source is located at the corner of the planes so that all modes are excited. The solid line shows the maximum radiated field strength at 10.0 m obtained from the complete expression in (13). The dashed line indicates the maximum estimate using (16). For this test board, the maximum level is expected to be determined by TM_{0n} modes because b is shorter than a . The results show that the maximum field intensity is determined by the TM_{01} and TM_{02} modes as expected and the estimate in (16) provides an upper bound for the maximum radiation.

Combining (14) and (16), a general expression for the maximum radiated field intensity from a power bus with a high Q

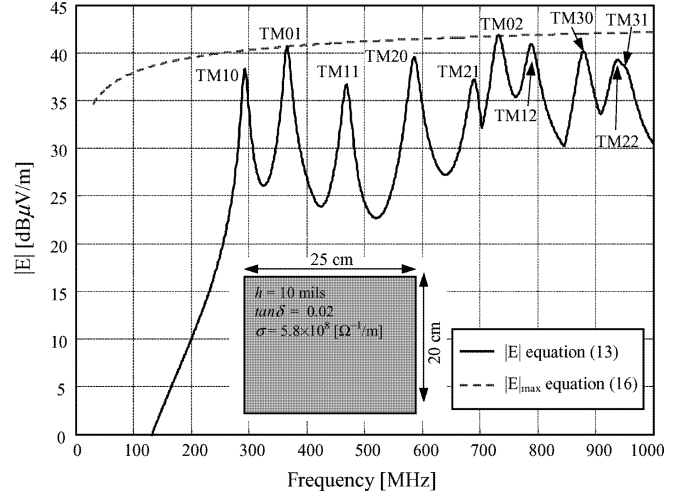


Fig. 3. Maximum radiation and corresponding modes at $r = 10$ m.

resonance is given by

$$|E|_{\max} \leq \frac{120hI_i}{\epsilon_r r} \cdot \frac{Q_{\text{bare}}(f)}{\min(a, b)}. \quad (17)$$

IV. RADIATION INTENSITY FROM A POPULATED BOARD

Equation (17) provides a simple closed-form estimate for the maximum radiated emissions from the power bus of a low loss board with high- Q resonances. If the board is heavily populated, the components introduce additional loss and the expression in (3) does not hold any more. In order to model the effects of components on a heavily populated board, we start by assuming the component loss is distributed uniformly over the board. The component loss is then accounted for by introducing an equivalent propagation constant. The new propagation constant, in turn, is used to get a closed-form expression for the maximum radiation from heavily populated power bus structures.

A. Modifying the Propagation Constant

If the spacing between the two planes is much smaller than the dimensions of the board, the electromagnetic fields propagate in a radial direction outward from the source. Based on this idea, an equivalent propagation constant within a power bus structure has been successfully obtained using a radial transmission line model [22], [28]. Fig. 4 illustrates the radial transmission line. As the wave propagates in the radial direction, the per-unit-length parameters vary with the distance ρ and are given by [22]

$$L(r) = \frac{\mu_0 h}{2\pi \rho} \quad (18)$$

$$C(r) = \frac{2\pi \epsilon_r \epsilon_0 \rho}{h} \quad (19)$$

$$R_r(r) = \frac{(1+j)}{\pi \sigma \delta_s \rho} \quad (20)$$

$$G_d(r) = \frac{2\pi \rho}{h} \omega \epsilon_r \epsilon_0 \tan \delta \quad (21)$$

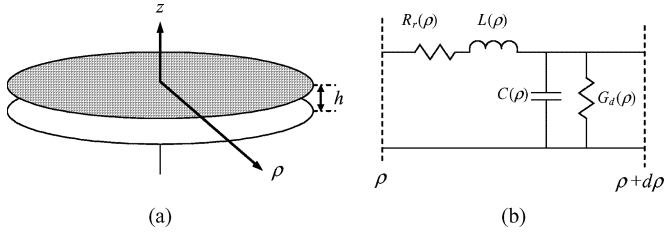


Fig. 4. (a) Geometry of the radial transmission line structure and (b) one segment of the radial transmission line model.

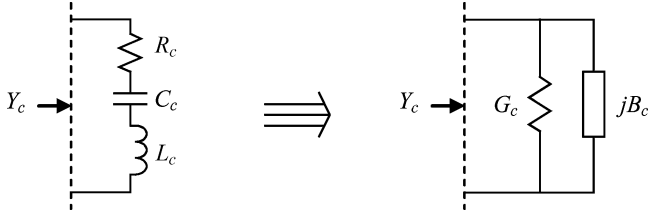


Fig. 5. High-frequency series and shunt models for a component.

Components connected to the two planes are in parallel with the shunt components of the model. A reasonable model for a component connected to the power planes of a printed circuit board is a series R - L - C as shown in Fig. 5. This could represent a passive linear component such as a lossy decoupling capacitor or the power input impedance of an active device. For a given series R_c , C_c , and L_c , a parallel connection that gives the same admittance is given by

$$G_c = \frac{R_c}{R_c^2 + \left(\omega L_c - \frac{1}{\omega C_c}\right)^2} \quad (22)$$

$$jB_c = -j \frac{\left(\omega L_c - \frac{1}{\omega C_c}\right)}{R_c^2 + \left(\omega L_c - \frac{1}{\omega C_c}\right)^2}. \quad (23)$$

Assuming that the number of the uniformly distributed components is N_c , the radial transmission line model can be modified as shown in Fig. 6. The per-unit length shunt parameters due to the connection of the components are given by

$$G_c(\rho) = \frac{2\pi\rho}{A} \cdot \frac{N_c R_c}{R_c^2 + \left(\omega L_c - \frac{1}{\omega C_c}\right)^2} \quad (24)$$

$$jB_c(\rho) = -j \frac{2\pi\rho}{A} \cdot \frac{N_c \left(\omega L_c - \frac{1}{\omega C_c}\right)}{R_c^2 + \left(\omega L_c - \frac{1}{\omega C_c}\right)^2} \quad (25)$$

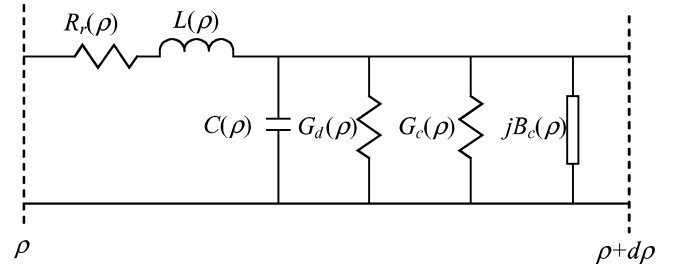


Fig. 6. Modified radial transmission line model including components.

where A is the area of the board. Using the above equations, a new propagation constant for the waves inside the cavity in the presence of components can be calculated from the series inductance and shunt admittance in Fig. 6, [22], [29] and is given by

$$\gamma = \sqrt{\{R_r(\rho) + j\omega L(\rho)\} \times \sqrt{\{G_d(\rho) + G_c(\rho) + j\omega C(\rho) + jB_c(\rho)\}}. \quad (26)$$

Substituting (18)–(21), (24), and (25) into (26) yields (27), shown at the bottom of the page, where $X_c(\omega) = \omega L_c - (\omega C_c)^{-1}$ and C_0 is the inter-plane capacitance of the power bus structure. Notice that (27) is identical to (3) if $N_c = 0$. For high-frequency signals, a resistor looks like a series R - L connection and a capacitor can be modeled as an equivalent R - L - C circuit. For typical printed circuit boards, decoupling capacitors resonate at tens of megahertz while the board resonances occur at hundreds of megahertz. At frequencies well above the decoupling capacitor resonant frequencies, transient currents are drawn primarily from the interplane capacitance [9]. At these frequencies, the trace inductance dominates and the capacitors look like resistances in series with inductances. Since the radiation from a power bus structure is usually only significant at frequencies near or above the first board resonance, the components can often be modeled using series R - L circuits for the purposes of power bus radiation estimation and $X_c(\omega)$ can be replaced simply by ωL_c . The radiated emissions from power bus structures are approximately proportional to the spacing between planes as indicated in (17) and significant only for thick boards, where the spacing h between the planes is much greater than the skin depth δ_s . In this case, (27) can be simplified as

$$\gamma^2 \approx -\omega^2 \mu_0 \varepsilon \left(\left[1 + \frac{\delta_s}{h} - \frac{N_c L_c}{C_0 (R_c^2 + \omega^2 L_c^2)} \right] - j \left[\tan \delta + \frac{\delta_s}{h} + \frac{N_c R_c}{\omega C_0 (R_c^2 + \omega^2 L_c^2)} \right] \right). \quad (28)$$

$$\gamma = j\omega \sqrt{\mu_0 \varepsilon} \times \sqrt{\left(1 - j \frac{(1+j)\delta_s}{h} \right)}$$

$$\times \sqrt{\left[\left(1 - \frac{N_c X_c(\omega)}{\omega C_0 |R_c + jX_c(\omega)|^2} \right) - j \left(\tan \delta + \frac{N_c R_c}{\omega C_0 |R_c + jX_c(\omega)|^2} \right) \right]}$$

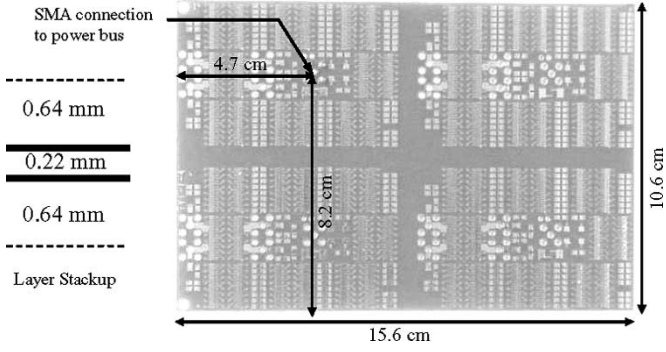


Fig. 7. Test board.

The complex propagation constant in (28) can be used in the cavity model to calculate the power bus impedance of a heavily populated board.

In order to validate this approach, the input impedance of a test board was measured and compared with the cavity model calculation. The test board was 15.6 cm \times 10.6 cm. It was a six-layer board with planes on layers 3 and 4 for power distribution. The planes were separated by a 0.22-mm dielectric material with an effective relative dielectric constant of 5.35 and a loss tangent of approximately 0.02 over the frequency range of interest. Fig. 7 shows the test board. Surface mount 39- Ω resistors were connected to the two power planes through traces with a parasitic inductance of 1.4 nH. Fifty-two resistors were uniformly distributed over the board. The power bus impedance was measured at the SMA port with an HP4291A impedance analyzer.

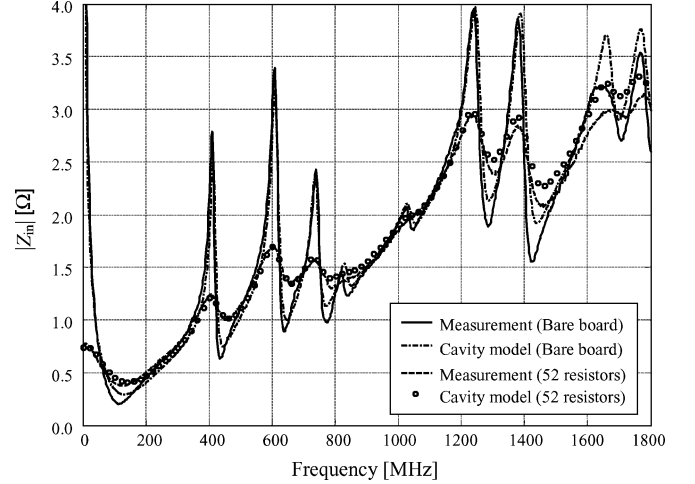
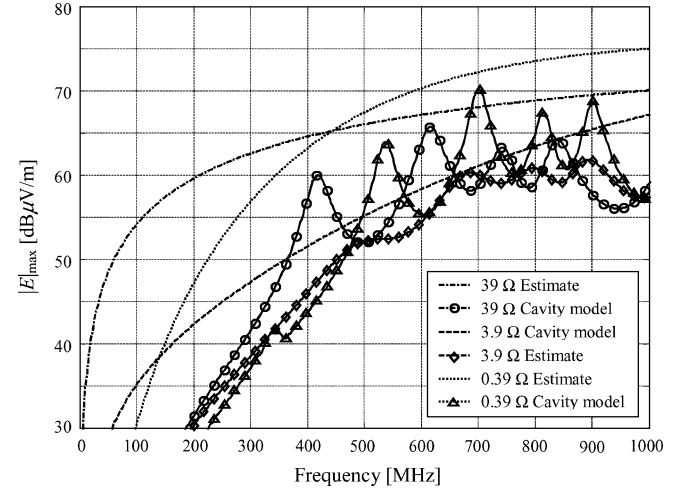
The power bus input impedance was calculated by setting $i = j$ in (1). The wave propagation constant in (28) was used to account for the effect of the components. The calculated and measured results are shown in Fig. 8. The measured values agree well with the calculation indicating that the modified wave propagation constant did a good job of accounting for the effects of the distributed components.

B. Estimation of the Maximum Emissions

Substituting (28) into (11) and (12), the radiated field can be calculated. As described in the previous section, the maximum field intensity is determined by the TM_{m0} or TM_{0n} modes. Considering the worst-case radiation, the maximum radiated field from a populated board can be written as

$$|E| \leq \frac{120hI_i}{\epsilon_r r \min(a, b)} \cdot \left(\tan \delta + \frac{\delta_s}{h} + \frac{N_c R_c}{\omega C_0 (R_c^2 + \omega^2 L_c^2)} \right)^{-1} \\ = \frac{120hI_i}{\epsilon_r r} \cdot \frac{Q(f)}{\min(a, b)}. \quad (29)$$

The estimates calculated using (29) are shown in Fig. 9 along with the simulated results using (13). The configuration of the test board was the same as that of the test board used for the impedance measurement earlier. The radiated field was calculated using the cavity model with 22 resistors connected between the planes. A filamentary 10-mA current source was placed at (4.7, 8.2) cm. The simulations show that the quality factor of

Fig. 8. Power bus impedance of the test board populated by 52 lumped resistors of 39 Ω with 1.4 nH of connection inductance.Fig. 9. Effect of component resistance on the radiated emissions ($N_c = 22$, $L_c = 1.4$ nH, $h = 0.22$ mm).

the resonance is relatively high when the resistor value is 39 Ω . The quality factor is also high when the resistor value is 0.39 Ω . However, with a resistance of 3.9 Ω , the quality factor is lower and the resonances are dampened more efficiently. This is because maximum power is delivered to the resistors when their resistance is equal to the inductive reactance of their connection to the board [30]. At frequencies in the hundreds of megahertz, a connection inductance of 1.4 nH has a reactance on the order of several ohms. Since the power bus impedance is also in the range of several ohms, the 3.9- Ω resistors are able to damp the power bus resonances effectively. The relatively high-impedance 39- Ω resistors and the relatively low-impedance 0.39- Ω resistors do not readily absorb power from the board.

Maximum levels of estimated radiation calculated using (29) are also illustrated in Fig. 9. The results indicate that this expression successfully estimates the maximum strength of the radiated emissions.

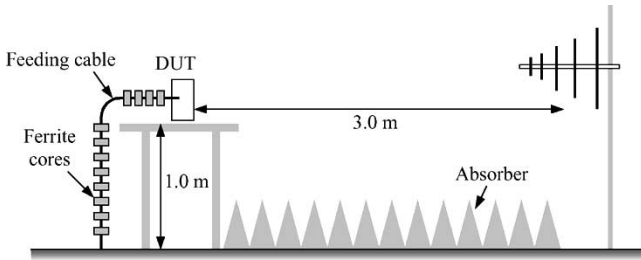


Fig. 10. Setup for measuring radiated emissions.

V. EXPERIMENTAL VALIDATION

In order to determine how well the simple expression in (29) estimates the maximum emissions from an actual printed circuit board, radiated emissions from the test board shown in Fig. 7 were measured in various configurations. Fig. 10 shows the measurement setup. The board was placed on a 1-m high table inside an anechoic chamber. The signal source was connected to the SMA port through a coaxial cable and the radiated fields were measured using a wide-band antenna. Several ferrite cores were placed on the coaxial cable to minimize the common-mode current induced on the cable. The maximum intensity of the electric field was measured as the table was rotated and the antenna height was varied. The board was measured both parallel and perpendicular to the plane of the table. The distance between antenna and the DUT was 3.0 m.

The measured radiated emissions from the bare board (without any components) are shown in Fig. 11 along with calculated emissions using the cavity model (13) and the estimated maximum emissions (29). The measured results show a small peak near 40 MHz that was associated with a cable resonance and appeared only when the antenna was oriented vertically. The results show that the cavity model predicts the intensity of the radiated emissions with reasonable accuracy and the closed-form expression for maximum radiation in (17) successfully estimates the envelope of the emissions. The fact that none of the peaks actually reach the maximum estimate can be attributed to the fact that the source location is not in a perfect position to strongly excite any of the resonances.

The radiated emissions from a populated board are shown in Fig. 12. Surface mount resistors with a nominal value of 39 Ω were connected to the power bus. The connection inductance was 1.4 nH and the resistors were distributed across the board.

Fig. 12(a) shows the results obtained with 22 resistors and Fig. 12(b) shows results obtained with 52 resistors mounted to the board. In both cases, the estimate given by (29) provides a reasonable upper-bound for the maximum radiation intensity. Note that the peaks are closer to the upper bound when there is significant loss. This is because the source location is less critical in a lossy cavity.

VI. CONCLUSION

A simple expression for the maximum radiated emissions from a populated parallel plane power bus structure was derived. In order to consider the effects of components on the

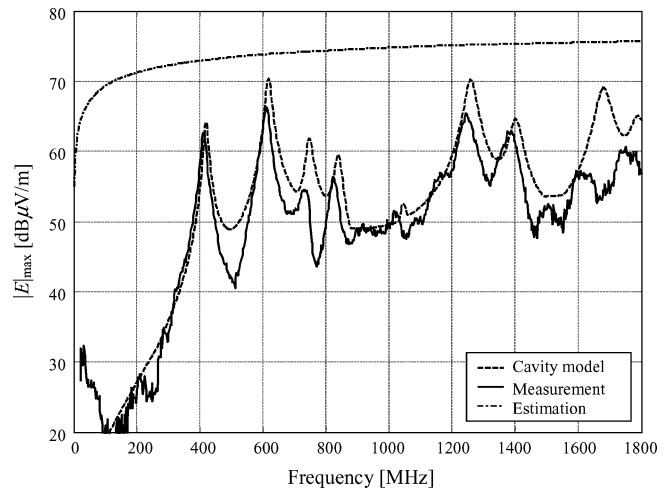
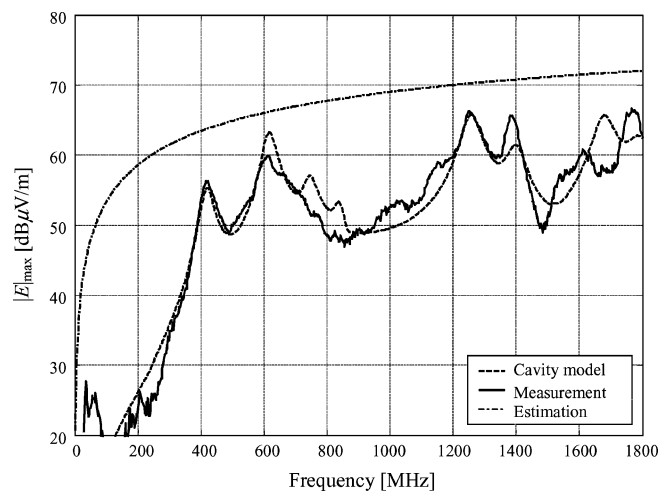
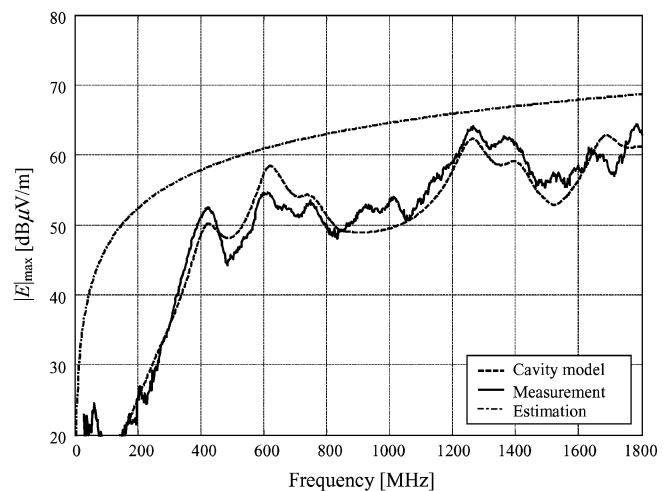


Fig. 11. Radiated emissions from a bare board.



(a)



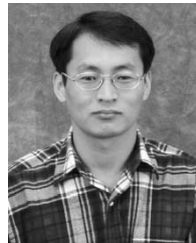
(b)

Fig. 12. Radiated emissions from a board populated with (a) 22 and (b) 52 39- Ω resistors.

board, rectangular power bus structures were analyzed using a cavity model and the complex wave propagation constant within the cavity was modified to take into account the effect of components. Measurements of the power bus impedance for a sample board populated with resistors to represent the ESR of active devices and decoupling capacitors showed good agreement with calculated results supporting the effectiveness of the model.

REFERENCES

- [1] S. Radu and D. Hockanson, "An investigation of PCB radiated emissions from simultaneous switching noise," in *Proc. IEEE Int. Symp. Electromag. Compat.*, Seattle, WA, Aug. 1999, pp. 893–898.
- [2] F. Gisin and Z. Pantic-Tanner, "Radiation from printed circuit board edge structures," in *Proc. IEEE Int. Symp. Electromag. Compat.*, Montreal, QC, Canada, Aug. 2001, pp. 881–883.
- [3] S. Haga, K. Nakano, and O. Hashimoto, "Reduction in radiated emission by symmetrical power-ground stack-up PCB with no open edge," in *Proc. IEEE Int. Symp. Electromag. Compat.*, Minneapolis, MN, Aug. 2002, pp. 262–267.
- [4] O. Mandhana, "Modeling, analysis and design of resonant free power distribution network for modern microprocessor systems," *IEEE Trans. Adv. Packag.*, vol. 27, no. 1, pp. 107–120, Feb. 2004.
- [5] B. Archambeault and A. Ruehli, "Analysis of power/ground-plane EMI decoupling performance using the partial-element equivalent circuit technique," *IEEE Trans. Electromagn. Compat.*, vol. 43, no. 4, pp. 437–445, Nov. 2001.
- [6] J. Fan, J. Drewniak, J. Knighten, N. Smith, A. Orlandi, T. Van Doren, T. Hubing, and R. DuBroff, "Quantifying SMT decoupling capacitor placement in dc power-bus design for multilayer PCBs," *IEEE Trans. Electromagn. Compat.*, vol. 43, no. 4, pp. 588–599, Nov. 2001.
- [7] L. Smith, R. Anderson, D. Forehand, T. Pelc, and T. Roy, "Power distribution system design methodology and capacitor selection for modern CMOS technology," *IEEE Trans. Adv. Packag.*, vol. 22, no. 3, pp. 284–291, Aug. 1999.
- [8] W. Becker, J. Eckhardt, R. Frech, G. Katopis, E. Klink, M. McAllister, T. McNamara, P. Muench, S. Richter, and H. Smith, "Modeling, simulation, and measurement of mid-frequency simultaneous switching noise in computer system," *IEEE Trans. Adv. Packag.*, vol. 21, no. 2, pp. 157–163, May 1998.
- [9] T. Hubing, J. Drewniak, T. Van Doren, and D. Hockanson, "Power bus decoupling on multilayer printed circuit boards," *IEEE Trans. Electromagn. Compat.*, vol. 37, no. 2, pp. 155–166, May 1995.
- [10] I. Novak, L. Noujeim, V. St Cyr, N. Biunno, A. Patel, G. Korony, and A. Ritter, "Distributed matched bypassing for board-level power distribution networks," *IEEE Trans. Adv. Packag.*, vol. 25, no. 2, pp. 230–24, May 2003.
- [11] M. Xu, T. Hubing, J. Chen, T. Van Doren, J. Drewniak, and R. DuBroff, "Power bus decoupling with embedded capacitance in printed circuit board design," *IEEE Trans. Electromagn. Compat.*, vol. 45, no. 1, pp. 22–30, Feb. 2003.
- [12] V. Ricchiuti, "Power-supply decoupling on fully populated high-speed digital PCBs," *IEEE Trans. Electromagn. Compat.*, vol. 43, no. 4, pp. 671–676, Nov. 2001.
- [13] I. Novak, "Reducing simultaneous switching noise and EMI on ground/power planes by dissipative edge termination," *IEEE Trans. Adv. Packag.*, vol. 22, no. 3, pp. 274–283, Aug. 1999.
- [14] X. Ye, D. Hockanson, M. Li, Y. Ren, W. Cui, J. Drewniak, and R. DuBroff, "EMI mitigation with multilayer power-bus stacks and via stitching of reference planes," *IEEE Trans. Electromagn. Compat.*, vol. 43, no. 4, pp. 538–548, Nov. 2001.
- [15] S. Haga, K. Nakano, and O. Hashimoto, "Reduction in radiated emission by symmetrical power-ground layer stack-up PCB with no open edge," in *Proc. IEEE Int. Symp. Electromag. Compat.*, Minneapolis, MN, Aug. 2002, pp. 262–267.
- [16] M. Leone, "The radiation of a rectangular power-bus structure at multiple cavity-mode resonances," *IEEE Trans. Electromagn. Compat.*, vol. 45, no. 3, pp. 486–492, Aug. 2003.
- [17] G.-T. Lei, R. Techentin, P. Hayes, D. Schwab, and B. Gilbert, "Wave model solution to the ground/power plane noise problem," *IEEE Trans. Instrum. Meas.*, vol. 44, pp. 300–303, Apr. 1995.
- [18] I. Novak, "Accuracy considerations of power-ground plane models," in *Proc. 8th Meeting on Electrical Performance of Electronic Packaging*, San Diego, CA, Oct. 1999, pp. 153–156.
- [19] S. Chun, M. Swaminathan, L. Smith, J. Srinivasan, Z. Jin, and M. Iyer, "Modeling of simultaneous switching noise in high speed systems," *IEEE Trans. Adv. Packag.*, vol. 24, pp. 132–142, May 2001.
- [20] G.-T. Lei, R. Techentin, and B. Gilbert, "High-frequency characterization of power/ground-plane structures," *IEEE Trans. Microw. Theory Tech.*, vol. 47, pp. 562–569, May 1999.
- [21] M. Xu, Y. Ji, T. Hubing, J. Drewniak, and T. Van Doren, "Development of a closed-form expression for the input impedance of power-ground plane structures," in *Proc. IEEE Int. Symp. Electromag. Compat.*, Washington, DC, Aug. 2000, pp. 77–82.
- [22] M. Xu, H. Wang, and T. Hubing, "Application of the cavity model to lossy power-return plane structures in printed circuit boards," *IEEE Trans. Adv. Packag.*, vol. 26, no. 1, pp. 73–80, Feb. 2003.
- [23] M. Xu and T. Hubing, "Estimating the power bus impedance of printed circuit boards with embedded capacitance," *IEEE Trans. Adv. Packag.*, vol. 25, no. 3, pp. 424–432, Aug. 2002.
- [24] Y. T. Lo, D. Solomon, and W. F. Richards, "Theory and experiment on microstrip antennas," *IEEE Trans. Antennas Propag.*, vol. 27, pp. 137–145, Mar. 1979.
- [25] C. A. Balanis, *Antenna Theory*, 2nd ed. New York: Wiley chs. 3 and 14, 1997.
- [26] W. L. Stutzmann and G. A. Thiele, *Antenna Theory and Design*. New York: Wiley, 1981.
- [27] R. F. Harrington, *Time-Harmonic Electromagnetic Fields*. New York: McGraw-Hill, 1961, ch. 3.
- [28] J. Parker, "Via coupling within parallel rectangular planes," *IEEE Trans. Electromagn. Compat.*, vol. 39, pp. 17–23, Feb. 1997.
- [29] S. Ramo and J. R. Whinnery, *Fields and Waves in Modern Radio*, 2nd ed., New York: Wiley, 1953.
- [30] T. Zeeff and T. Hubing, "Reducing power bus impedance at resonance with lossy components," *IEEE Trans. Adv. Packag.*, vol. 25, pp. 307–310, May 2002.



Hwan-Woo Shim (M'96) was born in Kyungpook Province, South Korea, in 1968. He received the B.E. degree from Kyungpook National University in 1991 and the M.S. degree from Korea Advanced Institute of Science and Technology (KAIST) in 1994. In 1999, he joined the EMC Laboratory, University of Missouri-Rolla, where he received the Ph.D. degree in electrical engineering in 2004.

From 1994 to 1999, he was with Electronics and Telecommunication Research Institute (ETRI), Daejeon, South Korea. Since 2004, he has been working for Samsung Electronics Co., where he develops GSM mobile phones. His research interests include electromagnetic compatibility problems, advanced RF measurements and computational electromagnetics.



Todd H. Hubing (S'82–M'82–SM'93) received the B.S.E.E. degree from the Massachusetts Institute of Technology, Cambridge, in 1980, the M.S.E.E. degree from Purdue University, West Lafayette, IN, in 1982, and the Ph.D. degree in electrical engineering from North Carolina State University, Raleigh, in 1988.

He is currently a Professor of Electrical Engineering with the University of Missouri-Rolla (UMR), where he is also a member of the Principal Faculty in the Electromagnetic Compatibility Laboratory. Prior to joining UMR in 1989, he was an Electromagnetic Compatibility Engineer with IBM, Research Triangle Park, NC. Since joining UMR, the focus of his research has been measuring and modeling sources of electromagnetic interference. He has authored or presented over 100 technical papers, presentations, and reports on electromagnetic modeling and electromagnetic compatibility related subjects.

Dr. Hubing was a Member of the Board of Directors of the IEEE EMC Society from 1995 to 2005 and is a Past President of the Society. He has also served as an Associate Editor of the IEEE TRANSACTIONS ON ELECTROMAGNETIC COMPATIBILITY and the *Journal of the Applied Computational Electromagnetics*.